



Numerical Approximation of Internal Temperature in the Cylinder of an IC Engine

G. Karamali, H. Dastoor

School of Basic Science, ShahidSattari University of Aeronautical Engineering, Tehran, Iran

gh_karamali@azad.ac.ir

School of Basic Science, ShahidSattari University of Aeronautical Engineering, Tehran, Iran

dastoormirkalaei@gmail.com

ABSTRACT

In this study, mollification and marching methods are used to solve an inverse problem in combustion engines. With the benefit of 2D mollification, we first propose an algorithm, and then prove some theorems, which ensure us the proposed method is stable and reliable, and then some numerical experiment has been done to show the efficiency of the method.

Indexing terms/Keywords

Inverse problems; Mollification method; Marching method; Combustion Engines.

Academic Discipline And Sub-Disciplines

Applied Mathematics;

SUBJECT CLASSIFICATION

65L09

TYPE (METHOD/APPROACH)

Mollification method and Marching method.

Council for Innovative Research

Peer Review Research Publishing System

Journal: JOURNAL OF ADVANCES IN MATHEMATICS

Vol.10, No.4

www.cirjam.com , editorjam@gmail.com



Introduction

Inverse problems play a vital role in science and engineering and have rightfully received a great deal of attention by applied mathematicians, statisticians, and engineers. The most interesting characteristic of inverse problems is that they cannot be solved analytically; hence how accurate we solve them by computational methods in another important task to do [4].

The majority of the methods that have been proposed for solving inverse problems were formalized in the last four decades in terms of their capabilities to treat ill-posed unstable problems. The basis of such formal methods resides on the idea of reformulating an inverse problem in terms of an approximate well-posed problem, by utilizing some kind of regularization techniques [1].

Following the model introduced in [1, 3], which the in-cylinder pressure in an internal combustion engine was modeled as a function of crank angle. In this article, we would like to consider the temperature as a function of crank angle and variation of piston in cylinder during the compression stroke. Basically, we aim to add more minute details to the problem of interest and generate an efficient numerical method to solve the problem.

For convenience we outline our procedure as follows:

In the next section, the *mathematical formulation* of our interest problem is described. The next section, the *regularized problem and the marching scheme* is described [2]. In the next section, a marching algorithm is generated to have the optimized solution. After that to prove the reliability of the proposed method, stability and convergence analysis are discussed. After that, for testing the method, two examples are discussed.

Description of the Problem

In internal combustions (IC) engines, the mathematical model of heat transfer process in cylinder wall in general form may be written as follows [1,3],

$$\frac{\partial^2 T}{\partial r^2} + \frac{1}{r} \frac{\partial T}{\partial r} + \frac{1}{r^2} \frac{\partial^2 T}{\partial \theta^2} + \frac{\partial^2 T}{\partial z^2} = k \frac{\partial T}{\partial t} \quad (1)$$

Where $T = T(r, z, t)$, $R_1 < r < R_2$, $0 < \theta < 2\pi$, $0 < z < a$ and $0 < t < T_c$. Also the boundary conditions regarding the problem may be written as follows

$$T(R_1, z, t) = P(t, z), \quad (2)$$

$$k \frac{\partial T}{\partial \theta}(R_2, z, t) = q(t, z), \quad (3)$$

$$\frac{\partial T}{\partial z}(r, 0, t) = \varphi(r, t), \quad (4)$$

$$\frac{\partial T}{\partial z}(r, b, t) = \psi(r, t), \quad (5)$$

$$T(r, b, 0) = f(r, t). \quad (6)$$

In cylinder one may consider that the variation of T is not dependent on θ . Therefore, in the equation (1), the term $\frac{\partial^2 T}{\partial \theta^2}$ can be dropped. On the other hand, the crank angle base of a lot of information in IC engines and it is clear that crank angle varies with time, i.e. $\alpha = \alpha(t)$, which implies,

$$\frac{\partial T}{\partial t} = \frac{\partial T}{\partial \alpha} \cdot \frac{\partial \alpha}{\partial t}. \quad (7)$$

In IC engines $\frac{\partial \alpha}{\partial t}$ defines the engine angular speed, ω_e , and it is considered as follows,

$$\frac{\partial \alpha}{\partial t} = \omega_e = \frac{2\pi N}{60}, \quad (8)$$

Where N demonstrates the engine speed. We can rewrite equation (1) using equation (8), we have

$$K \omega_e \frac{\partial T}{\partial \alpha} = \frac{\partial^2 T}{\partial r^2} + \frac{1}{r} \frac{\partial T}{\partial r} + \frac{\partial^2 T}{\partial z^2}, \quad (9)$$

Where the initial and boundary conditions may be written as follows,

$$T(R_1, z, \alpha) = P(z, \alpha), \quad (10)$$

$$K \frac{\partial T}{\partial r}(R_2, z, \alpha) = 0, \quad (11)$$

$$K \frac{\partial T}{\partial z}(r, 0, \alpha) = 0, \quad (12)$$

$$K \frac{\partial T}{\partial z}(r, b, 0) = f_1(r, b) \quad (13)$$

In the practical experiences, occasionally, the boundary conditions or some parts of them may be unavailable due to physical situations. Hence having an alternative condition to solve the problem is essential.



$$T(R_2, z, \alpha) = \eta(t), \tag{14}$$

The problem of interest, then, can be summarized as follows:

$$K\omega_e \frac{\partial u}{\partial \alpha} = \frac{\partial^2 u}{\partial r^2} + \frac{1}{r} \frac{\partial u}{\partial r} + \frac{\partial^2 u}{\partial z^2}, \tag{15}$$

$$T(R_1, z, \alpha) = P(z, \alpha) \tag{16}$$

$$T(R_2, z, \alpha) = \eta(z, \alpha), \tag{17}$$

$$K \frac{\partial v}{\partial r}(R_2, z, \alpha) = 0, \tag{18}$$

Where $K\omega_e$ is given and $\eta(t)$ is measured and also. Determining $v(r, z, \alpha)$ and $P(z, \alpha)$ from the problem is our primal goal. Furthermore, the known data function $\eta(z, \alpha)$ is only known approximately as $\eta^\epsilon(z, \alpha)$ such that

$$\|\eta(z, \alpha) - \eta^\epsilon(z, \alpha)\| \leq \epsilon \tag{19}$$

Where ϵ is a positive tolerance.

Regularized problem and the marching scheme

The mollified problem

The regularized problem, based on mollification, is formulated as follows.

$$K\omega_e \frac{\partial v}{\partial \alpha} = \frac{\partial^2 v}{\partial r^2} + \frac{1}{r} \frac{\partial v}{\partial r} + \frac{\partial^2 v}{\partial z^2}, \tag{20}$$

$$v(R_1, z, \alpha) = P(z, \alpha) \tag{21}$$

$$v(R_2, z, \alpha) = J_{\delta_1} \eta^\epsilon(z, \alpha), \tag{22}$$

$$K \frac{\partial v}{\partial r}(R_2, z, t) = 0, \tag{23}$$

where $v(r, z, \alpha)$ and $P(z, \alpha)$ are needed to be determined.

Marching scheme

Let $M, N,$ and $O,$ positive integers, $h = R_2 - R_1/M, l = a/O, k = 1/T_t$ be the parameters of the finite differences discretization. We introduce the discrete functions $U_{i,j}^n, Q_{i,j}^n, W_{i,j}^n, P_{i,j}^n$ and $S_{i,j}^n$ as discrete computed approximations of $v(ih, jl, nk), v_r(ih, jl, nk), v_\alpha(ih, jl, nk), v_z(ih, jl, nk)$ and $v_{zz}(ih, jl, nk)$ respectively. Then, the space marching algorithm is defined as follows.

1. Select δ_0 .
2. Perform mollification of η^ϵ and set.

$$U_{M,j}^n = J_{\delta_0} \eta^\epsilon(jl, nk), Q_{M,j}^n = 0.$$

3. Perform mollified differentiations. Set

$$U_{M,j}^n = \mathbf{D}_\alpha (J_{\delta_0} \eta^\epsilon(jl, nk)), S_{M,j}^n = \mathbf{D}_z (J_{\delta_0} U_{M,j}^n).$$

4. Initialize $i = M$. Do while $i \geq 1$,

- i. $U_{i-1,j}^n = U_{i,j}^n - h Q_{i,j}^n,$ (24)

- ii. $Q_{i-1,j}^n = Q_{i,j}^n - h [K\omega_e W_{i,j}^n + \frac{1}{ih} Q_{i,j}^n + S_{i,j}^n],$ (25)

- iii. $W_{i-1,j}^n = W_{i,j}^n - h \mathbf{D}_\alpha (J_{\delta_i} Q_{i,j}^n),$ (26)

- iv. $P_{i-1,j}^n = P_{i,j}^n - k \mathbf{D}_z (J_{\delta_i} W_{i,j}^n),$ (27)

- v. $S_{i-1,j}^n = \mathbf{D}_z (J_{\delta_i} P_{i-1,j}^n).$ (28)

where \mathbf{D}_α and \mathbf{D}_z respectively denote the centered difference operator with respect to α and z [5]. From now on, we denote $|Y_i| = \max_{j,n} |Y_{i,j}^n|$ and $\|Y\|_\infty = \max_i |Y_i|$.

Stability and Convergence of the Scheme

In this section, we analyze the stability of the marching scheme (24)–(28). Without loss of generality, from now on, we assume $|\delta|_{-\infty} = \min\{\delta_i\}$, also $|Y_i| = \max_{j,n} |Y_{i,j}^n|$ and $\|Y\|_\infty = \max_i |Y_i|$.

Assumption 1: For all $(r, z, \alpha) \in I = [R_1, R_2] \times [0, l] \times [0, 2\pi]$, we further assume that $T(r, z, \alpha) \in C^2(I)$.

Theorem 1 [Stability]: If Assumption 1 holds, for the marching scheme (24)–(28), there exists a constant A , dependent on $|\delta|_{-\infty}$, such that



$$\max\{|U_0|, |Q_0|, |W_0|, |P_0|, |S_0|\} \leq \Lambda \max\{|U_M|, |Q_M|, |W_M|, |P_M|, |S_M|\}.$$

Proof:

Using theorem 4 and 6 from [5], there exist constants C_1, C_2 and C_3 such that,

$$\mathbf{D}_\alpha(Q_{i,j}^n) \leq \frac{C_1}{|\delta|^{-\infty}} |Q_i|, \mathbf{D}_z(W_{i-1,j}^n) \leq \frac{C_2}{|\delta|^{-\infty}} |W_i| \text{ and } \mathbf{D}_z(P_{i-1,j}^n) \leq \frac{C_3}{|\delta|^{-\infty}} |P_i| \tag{29}$$

We have from (24)-(26) and (29)

$$|U_{i-1,j}^n| \leq |U_{i,j}^n| + h|Q_{i,j}^n| \leq (1 + h) \max\{|U_i|, |Q_i|\} \tag{30}$$

$$\begin{aligned} |Q_{i-1,j}^n| &\leq |Q_{i,j}^n| + h \left[K\omega_e |W_{i,j}^n| + \frac{1}{ih} |Q_{i,j}^n| + |S_{i,j}^n| \right] \leq |Q_{i,j}^n| + h[K\omega_e |W_{i,j}^n| + \xi |Q_{i,j}^n| + |S_{i,j}^n|] \\ &\leq (1 + C_q h) \max\{|W_i| + |Q_i| + |S_i|\}. \end{aligned} \tag{31}$$

$$|W_{i-1,j}^n| \leq |W_i| + h \frac{C_1}{|\delta|^{-\infty}} |Q_i| \leq \left(1 + h \frac{C_1}{|\delta|^{-\infty}}\right) \max\{|Q_i|, |W_i|\}. \tag{32}$$

Also,

$$|P_{i-1,j}^n| \leq |P_{i,j}^n| + h \frac{C_2}{|\delta|^{-\infty}} |W_{i,j}^n| \leq \left(1 + h \frac{C_2}{|\delta|^{-\infty}}\right) \max\{|P_i|, |W_i|\} \tag{33}$$

$$|S_{i-1,j}^n| \leq \frac{C_3}{|\delta|^{-\infty}} |P_{i-1,j}^n| \leq \left(h \frac{C_3}{|\delta|^{-\infty}}\right) \max\{|P_i|\} \tag{34}$$

Now let $C_\delta = \left\{1, C_q, \frac{C_1}{|\delta|^{-\infty}}, \frac{C_2}{|\delta|^{-\infty}}\right\}$, then from (30)-(34) we can conclude,

$$\max\{|U_{i-1}|, |Q_{i-1}|, |W_{i-1}|, |P_{i-1}|, |S_{i-1}|\} \leq (1 + C_\delta h) \max\{|U_i|, |Q_i|, |W_i|, |P_i|, |S_i|\}, \tag{35}$$

and iterating this last inequality M times, we have

$$\max\{|U_0|, |Q_0|, |W_0|, |P_0|, |S_0|\} \leq (1 + C_\delta h)^M \max\{|U_M|, |Q_M|, |W_M|, |P_M|, |S_M|\} \tag{36}$$

which implies

$$\max\{|U_0|, |Q_0|, |W_0|, |P_0|, |S_0|\} \leq \exp(C_\delta) \max\{|U_M|, |Q_M|, |W_M|, |P_M|, |S_M|\} \tag{37}$$

Setting $\Lambda = \exp(C_\delta)$ completes the proof of this statement.

We will now show that the above scheme convergence to the desired $J_\delta v$ for fixed δ . To do so, we define

$$\begin{aligned} \Delta U_{i,j}^n &= U_{i,j}^n - v(ih, jl, nk), & \Delta Q_{i,j}^n &= Q_{i,j}^n - v_r(ih, jl, nk), & \Delta W_{i,j}^n &= W_{i,j}^n - v_\alpha(ih, jl, nk), \\ \Delta P_{i,j}^n &= P_{i,j}^n - v_z(ih, jl, nk), & \Delta S_{i,j}^n &= S_{i,j}^n - v_{zz}(ih, jl, nk), \end{aligned}$$

and denote $\Delta_i = \max\{\Delta U_i, \Delta Q_i, \Delta W_i, \Delta P_i, \Delta S_i\}$.

From the marching scheme introduced in (24)–(28), we can notice that the mollified solution $v(r, z, \alpha)$ satisfies

$$v((i-1)h, jl, nk) = v(ih, jl, nk) - hv_r(ih, jl, nk), \tag{38}$$

$$v_r((i-1)h, jl, nk) = v_r(ih, jl, nk) - h \left[K\omega_e v_\alpha(ih, jl, nk) + \frac{1}{ih} v_r(ih, jl, nk) + \frac{\partial}{\partial z} v_z(ih, jl, nk) \right], \tag{39}$$

$$v_\alpha((i-1)h, jl, nk) = v_\alpha(ih, jl, nk) - h \frac{\partial}{\partial \alpha} v_r(ih, jl, nk), \tag{40}$$

$$v_z((i-1)h, jl, nk) = v_z(ih, jl, nk) - h \frac{\partial}{\partial z} v_\alpha(ih, jl, nk), \tag{41}$$

$$v_{zz}((i-1)h, jl, nk) = \frac{\partial}{\partial z} v_z((i-1)h, jl, nk), \tag{42}$$

Comparing (38)-(42) with the scheme, we can write

$$\begin{aligned} \Delta U_{i-1,j}^n &= \Delta U_{i,j}^n + (U_{i-1,j}^n - U_{i,j}^n) - \left(v((i-1)h, jl, nk) - v(ih, jl, nk) \right) + O(h^2), \\ &= \Delta U_{i,j}^n + h\Delta Q_{i,j}^n + O(h^2), \end{aligned} \tag{43}$$

$$\begin{aligned} \Delta Q_{i-1,j}^n &= \Delta Q_{i,j}^n + (Q_{i-1,j}^n - Q_{i,j}^n) - \left(v_r((i-1)h, jl, nk) - v_r(ih, jl, nk) \right) + O(h^2), \\ &= \Delta Q_{i,j}^n - h \left[K\omega_e \Delta W_{i,j}^n + \frac{1}{ih} \Delta Q_{i,j}^n + \Delta S_{i,j}^n \right] + O(h^2), \end{aligned} \tag{44}$$

$$\begin{aligned} \Delta W_{i-1,j}^n &= \Delta W_{i,j}^n - h \left(v_\alpha((i-1)h, jl, nk) - v_\alpha(ih, jl, nk) \right) + O(h^2), \\ &= \Delta W_{i,j}^n - h \left[\mathbf{D}_\alpha(J_{\delta_i} Q_{i,j}^n) - v_{r\alpha}(ih, jl, nk) \right] + O(h^2), \end{aligned} \tag{45}$$



$$\begin{aligned} \Delta P_{i-1,j}^n &= \Delta P_{i,j}^n - h(v_z((i-1)h, jl, nk) - v_z(ih, jl, nk)) + O(h^2), \\ &= \Delta W_{i,j}^n - h[D_z(J_{\delta_i'} W_{i-1,j}^n) - v_{\alpha z}(ih, jl, nk)] + O(h^2), \end{aligned} \tag{45}$$

Also

$$|U_{i-1,j}^n| \leq |\Delta U_{i,j}^n| + h|\Delta Q_{i,j}^n| + O(h^2), \tag{47}$$

$$|\Delta Q_{i-1,j}^n| \leq |\Delta Q_{i,j}^n| + h[K\omega_e |\Delta W_{i,j}^n| + \frac{1}{ih} |\Delta Q_{i,j}^n| + |\Delta S_{i,j}^n|] + O(h^2). \tag{48}$$

Using theorem 4 and 6 from [5], we have

$$|\Delta W_{i-1,j}^n| \leq |\Delta W_{i,j}^n| + h\left(\frac{C}{|\delta|_{-\infty}} (|\Delta Q_{i,j}^n| + k) + C_\delta k^2\right) + O(h^2), \tag{49}$$

$$|\Delta P_{i-1,j}^n| \leq |\Delta P_{i,j}^n| + h\left(\frac{C}{|\delta|_{-\infty}} (|\Delta W_{i,j}^n| + l) + C_\delta l^2\right) + O(h^2). \tag{50}$$

Letting $C_0 = \{1, K\omega_e + 2\}$ and $C_1 = \left\{\frac{Ck}{|\delta|_{-\infty}} + C_\delta k^2, \frac{Cl}{|\delta|_{-\infty}} + C_\delta l^2\right\}$

$$|\Delta_{i-1}| \leq (1 + C_0 h)|\Delta_i| + O(h^2). \tag{51}$$

By calculating L iterations,

$$\Delta_L \leq \exp\left(\frac{C r_L}{|\delta|_{-\infty}^2}\right) (\Delta_0 + C(l + k + h)). \tag{52}$$

Since

$$\Delta_M \leq \frac{C}{|\delta|_{-\infty}^2} (\varepsilon + l + k), \tag{53}$$

the convergence of the algorithm readily follows. That is Δ_L converges to zero as ε, h, k and l tend to zero.

Numerical Results

In this section to show the ability of the proposed numerical procedure, we present two examples. In all cases, without loss of generality, we set $p = 3$ (see [2]). The radii of mollification are always chosen automatically using the mollification and GCV methods. Discretized measured approximations of boundary data are modeled by adding random errors to the exact data functions. For example, for the boundary data function $h(x, t)$, its discrete noisy version is generated by

$$h_{j,n}^\varepsilon = h(x_j, t_n) + \varepsilon_{j,n}, j = 0, 1, \dots, N, n = 0, 1, \dots, T, \tag{54}$$

where the $\varepsilon_{j,n}$ are random variables uniformly distributed on $[-\varepsilon, \varepsilon]$.

The errors exact and approximate solution are measured by the relative RMS-norm.

Example 1: As the first example, in equations (15)-(18) consider $K = 1, \omega_e = 2.576$ and $\eta(z, \alpha) = e^{-0.08} \sin \alpha + z^2$. Also, $R_1 = 0.02, R_2 = 0.08, a = 0.15$ and $T_t = 2$.

Since this problem cannot be solved analytically, we follow a scheme which compares the solutions with each other.

Table 1 demonstrates RMS norm of comparing two solutions at three different mesh levels and two different amounts of ε .

Table 1. Comparing solutions with each other

| $M = N = O$ | | ε | $\ P(z, \alpha) _{M_1} - P(z, \alpha) _{M_2}\ $ |
|-------------|-------|---------------|-------------------------------------------------|
| M_1 | M_2 | | |
| 128 | 256 | 0.01 | 0.0831 |
| 256 | 512 | 0.01 | 0.0698 |
| 512 | 1024 | 0.01 | 0.0357 |
| 128 | 256 | 0.05 | 0.0936 |
| 256 | 512 | 0.05 | 0.0908 |
| 512 | 1024 | 0.05 | 0.0806 |

Figure 1 illustrates the difference between two levels of noise at $M = 1024$ and for a fixed z .

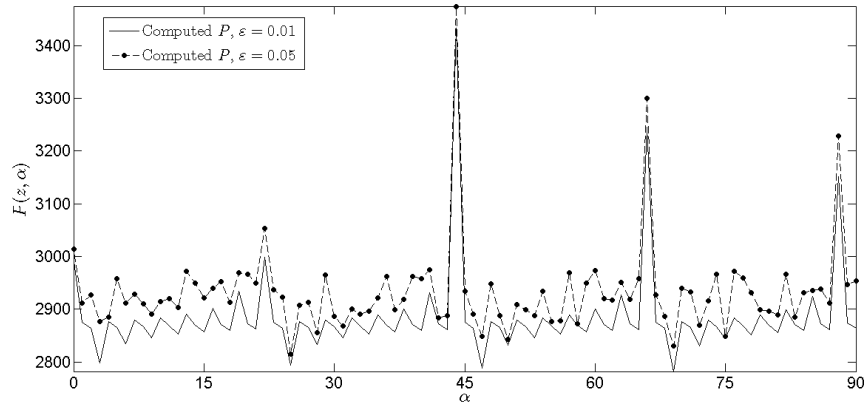


Fig 1: the difference between two levels of noise at $M = 1024$ and for a fixed z .

Example 2: In equations (15)-(18) consider $K = 1$, $\omega_e = 2.576$ and $\eta(z, \alpha) = e^z \cos \alpha$. Also, $R_1 = 0.02, R_2 = 0.1, a = 0.13$ and $T_t = 2.4$.

Table 2 demonstrates RMS norm of comparing two solutions at three different mesh levels and two different amounts of ϵ .

Table 2. Comparing the solution with each other

| $M = N = O$ | | ϵ | $\ P(z, \alpha) _{M_1} - P(z, \alpha) _{M_2}\ $ |
|-------------|-------|------------|-------------------------------------------------|
| M_1 | M_2 | | |
| 128 | 256 | 0.01 | 0.0809 |
| 256 | 512 | 0.01 | 0.0782 |
| 512 | 1024 | 0.01 | 0.0719 |
| 128 | 256 | 0.05 | 0.1058 |
| 256 | 512 | 0.05 | 0.0957 |
| 512 | 1024 | 0.05 | 0.0881 |

Figure 1 illustrates the difference between two levels of noise at $M = 1024$ and for a fixed z .

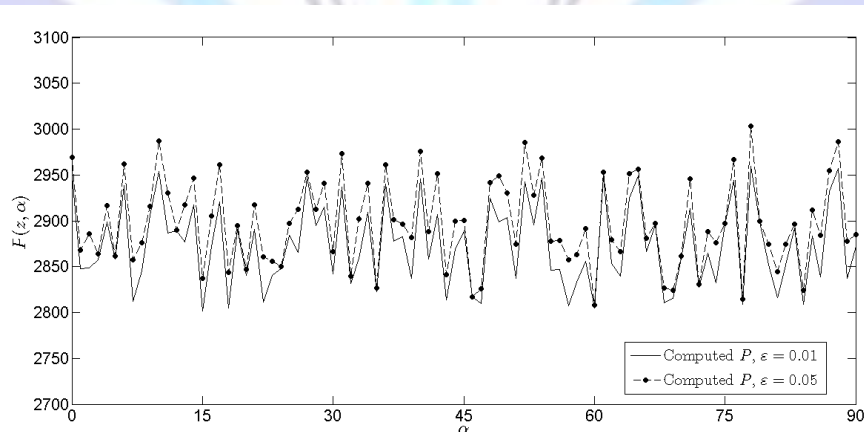


Fig 2: the difference between two levels of noise at $M = 1024$ and for a fixed z .

Conclusion

Overall, we developed a convergence scheme and it demonstrated a reasonable amount of accuracy, although analytical solutions were not available. This conclusion is consistent with the previous studies on this subject of interest [1, 3].



REFERENCES

- [1] Fakhraie M., Shidfar A., Garshasbi M. 2007A computational procedure for estimation of an unknown coefficient in an inverse boundary value problem, Applied Mathematics and Computation, Volume 187, Issue 2, , Pages 1120-1125, ISSN 0096-3003.
- [2] Murio D.A. 1993 The Mollification Method and the Numerical Solution of Ill-Posed Problems, John Wiley & Sons.
- [3] Shidfar A., Garshasbi M. 2005Numerical study of in-cylinder pressure in an internal combustion engine, Applied Mathematics and Computation, Volume 165, Issue 1, , Pages 163-170, ISSN 0096-3003.
- [4] Vogel, C.2002. Frontiers in Applied Mathematics, Society for Industrial and Applied Mathematics.
- [5] Yi Zh., Murio D.A. 2004Source term identification in 1-D IHCP, Computers & Mathematics with Applications, Volume 47, Issue 12, , Pages 1921-1933, ISSN 0898-1221.

